TAO, Vol. 10, No. 4, 805-820, December 1999

The ROCSAT-1 IPEI Preliminary Results: Vertical Ion Drift Statistics

Huey Ching Yeh[1], Shin-Yi Su[1], Roderick A. Heelis[2] and Jing-Mei Wu[1]

(Manuscript received 25 September 1999, in final form 5 November 1999)

ABSTRACT

We analyze the ROCSAT-1 IPEI data collected between March and June 1999 to study the statistical features of the ion vertical drifts at equatorial and tropical latitudes. The dependencies of ion vertical drifts on local time, longitude and geomagnetic field configuration, as well as geomagnetic activity are examined. The variations of the equatorial vertical drifts near the dawn and dusk terminators are of particular interest. From this preliminary study, we have shown that the overall local-time characteristics of the quiet-time equatorial vertical drift patterns derived from IPEI are in good agreement with those observed by other satellites and ground-based instruments. More importantly, several new results due to the unique 35° orbital inclination of ROCSAT-1 and the 100% duty-cycle operation of IPEI are found. These include: (a) enhanced upward ion drifts to a critical level of 30-60 m/s at post-sunset hours strongly correlate with the occurrence of rising bubbles in the pre-midnight local time sector; (b) large (> 300 m/s) downward ion drifts are most often found near sunrise and at longitudes where the geomagnetic field has greatest variations; (c) the statistical drift patterns strongly depend on the hemispheres at the equatorial anomaly latitudes. This north-south asymmetry may result from seasonal effects and/or from differences in geomagnetic field configuration.

(Key words: Prereversal enhancement, Equatorial plasma bubble, Sunrise ion drift, Equatorial anomaly ion motion)

1. INTRODUCTION

The ROCSAT-1 mission is taking place during the active phase of Solar Cycle 23. As ROCSAT-1 is maintained in a circular orbit at an altitude of 600 kilometers, and an orbital inclination of 35 degrees, observations with global coverage in local time and longitude are available every 52 days. The on board Ionospheric Plasma and Electrodynamics Instrument

[1]Institute of Space Science, National Central University, Chung-Li, Taiwan, ROC
[2]William B. Hanson Center for Space Science, University of Texas at Dallas, Richardson, Texas, USA

(IPEI) consists of 4 sensors to take in-situ measurements of ion density, temperature, composition and drift velocity over a large dynamic range with high sensitivity. Furthermore, since the IPEI payload is normally operated with a 100% duty cycle, the ROCSAT-IPEI can provide a fairly complete set of ion drift data for the low-latitude ionosphere during its mission lifetime. We therefore plan to use the ROCSAT-IPEI data set to compile a global electric field model for the solar maximum condition. The standard approach to develop an empirical model is to first find the statistical patterns and their controlling parameters. Since many reports concerning the statistical characteristics of equatorial ion vertical drifts have been published [e.g., Coley et al., 1989; Fejer et al., 1995; and Scherliess and Fejer, 1999], we focus on the vertical drift statistics for direct comparison with these reports. As the first step of developing a global electric field model at an altitude of 600 km, we analyze four months of ion velocity data from ROCSAT-IPEI to study the statistical patterns.

2. INSTRUMENT AND ION DRIFT VECTOR

The IPEI instrument consists of two packages: the Sensor Electronics Package (SEP) and the Main Electronics Package (MEP). The SEP contains an ion trap (IT), two ion drift meters (IDM), a retarding potential analyzer (RPA), and associated sensor electronics. The MEP contains a data processing unit, power supply, and spacecraft interface circuits. Figure 1 delineates the system configuration of the IPEI payload. The design of the IPEI drift meters is similar to those flown on the AE and DE satellites. The principles of the measurement technique used by the University of Texas at Dallas (UTD) to develop the IPEI drift meters have been reviewed by Hanson and Heelis [1975]. As shown in Fig. 1, the instrument (IPEI) frame of reference is defined: the positive X-axis in the ram direction of the IPEI aperture plane, the positive Z-axis in the nadir (pointing radially inward to the Earth) and the Y-axis complete a right-handed coordinate system. The ion drift meter measures arrival angles of ions with respect to the sensor looking direction (i.e., the positive X-axis of the IPEI coordinate frame). The two ion drift meters are placed along the Y-axis of the IPEI Y-Z plane. The +Y drift meter (+YDM) and -Y drift meter (-YDM) are physically identical and either one can be configured to measure either the horizontal (V_y) or vertical (V_z) drift component or to alternate between the two. The derivations of V_y and V_z from arrival angle measurements can be found in the report by Yeh [1998]. Combining V_y and V_z measurements with V_x derived from the RPA data the ion drift vectors in the IPEI frame of reference can be obtained.

To study the ionospheric electrodynamics, it will be frequently desirable to resolve the observed ion drifts into their components, which are parallel and perpendicular to the magnetic field. It is also important to describe the ion drifts in terms of their components, which are parallel to the east-west, north-south, and up-down directions of the geodetic coordinates, for the convenience of comparison with vast numbers of observations from ground-based instruments. Converting an ion drift vector in the sensor frame to that in the geodetic (geographic) coordinate frame requires rotation matrices that can remove the imperfect alignment between IPEI and the spacecraft body, the contributions of satellite motion and the contribution of corotation with the Earth.

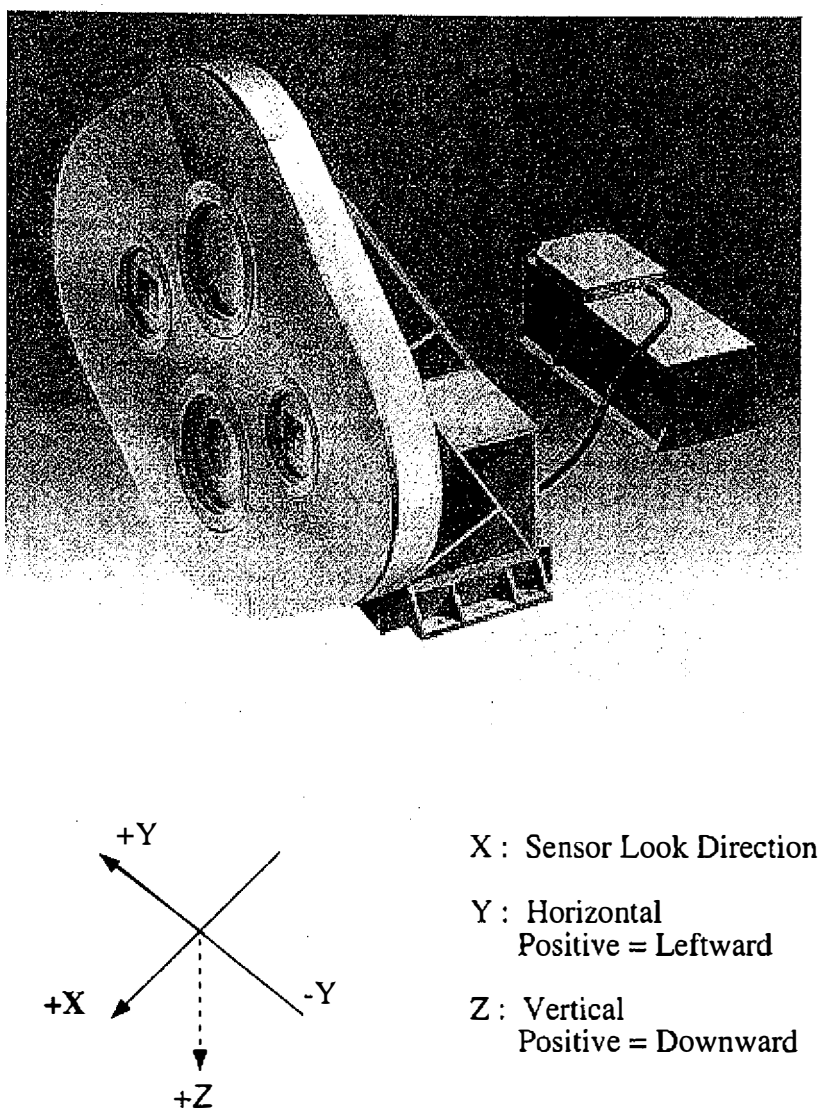

Fig. 1. System configuration of the IPEI payload with the sensor electronic package (SEP) on the left and the main electronic package (MEP) on the right. The instrument coordinates are defined as shown at the bottom of the figure. An observer facing the instrument sees "+Y" towards the left and "+Z" downwards. The two drift meters are along the Y-axis. The ion trap (IT) and RPA (at +Z) are along the Z-axis.

Figure 2 summarizes the required coordinate transforms from/to the IPEI reference frame. As the IPEI sensor was aligned within 0.5 degree of the three spacecraft reference axes, the small deviations between the instrument coordinate system (IPEI) and the spacecraft bus coordinate system (SBC) do not significantly affect the ion drift measurements. To remove the contributions of the satellite attitude motion, we need to transform the IPEI ion drift vectors to those in terms of the RPY coordinates. The Roll-Pitch-Yaw (RPY) coordinate system is an orbit-defined coordinate system, and is also called the Local Vertical / Local Horizontal (LVLH) system. The coordinates of this system maintain their orientations relative to the Earth as the spacecraft moves in its orbit. The three axes of the RPY system are defined as follows: the yaw-axis is directed toward the nadir; the pitch-axis is directed to the negative orbit normal; and the roll-axis is perpendicular to the other two. In a perfectly circular orbit, the roll axis is along the spacecraft velocity vector. The roll, pitch, and yaw angles (r, p, y) are defined as the right-handed rotations about their respective axes. The temporal variations of these Euler angles (r, p, y) describe the spacecraft attitude motion, and are controlled to be less than 0.1 degrees for the ROCSAT-1. When the Euler angles are known, the rotation matrix can be constructed for the coordinate transform between the SBC and RPY systems. The construction of the rotation matrix that relates the RPY coordinates to those of the Earth-centered inertial (ECI) coordinate system requires the satellite velocity and position vectors to be known in the ECI system. The contributions of satellite motion can be completely removed when the IPEI drift vectors are transformed into the ECI drift vectors. Further coordinate transform into the Earth-centered fixed (ECF) coordinate system is required to remove the Earth corotation contribution to the IPEI drift vectors. As discussed in Su et al. [1999], the corotation contribution to the IPEI V_y can be calculated using their Equation (1), and has the maximum value of 293 m/s at the equator and zero contribution in the high-latitude extremes ($\pm 35^o$) of the satellite orbit. The corotation has essentially no effect on the IPEI V_z measurement since it has no radial component. In a circular orbit, the contribution of satellite motion to the IPEI V_z measurement is also negligible if the attitude motion is well controlled.

Using the orbit and attitude data files provided by the Science Control Center (SCC) of the National Space Program Office (NSPO), we are able to construct the rotation matrices required to perform the coordinate transforms outlined in Fig. 2 to the ECF or the geodetic (GED) coordinate system. Furthermore, the geomagnetic field vectors in terms of GED (or ECF) coordinates can be derived from the updated International Geomagnetic Reference Field (IGRF95) model. The decomposition of the GED (or ECF) drift vectors into their components parallel (V_{para}) and perpendicular (V_{perp}) to the magnetic field vectors can then be performed.

As discussed above, the corresponding ion drift vectors in other coordinate systems of interest can be easily derived when the rotation matrices between them are known. However, the resolution of V_x data depends on the period of the RPA retarding potential sweep cycle, which has a typical resolution of two data points per second. Moreover, since V_x is one of several parameters to be inferred from a nonlinear modeling of an RPA I-V curve, it may be fixed at an estimated value when the I-V curve exhibits H^+ rich characteristics. In such case that the V_x data is not available, it will be necessary to make assumptions to complete the transform of an ion drift vector in terms of IPEI coordinates into one in terms of geodetic

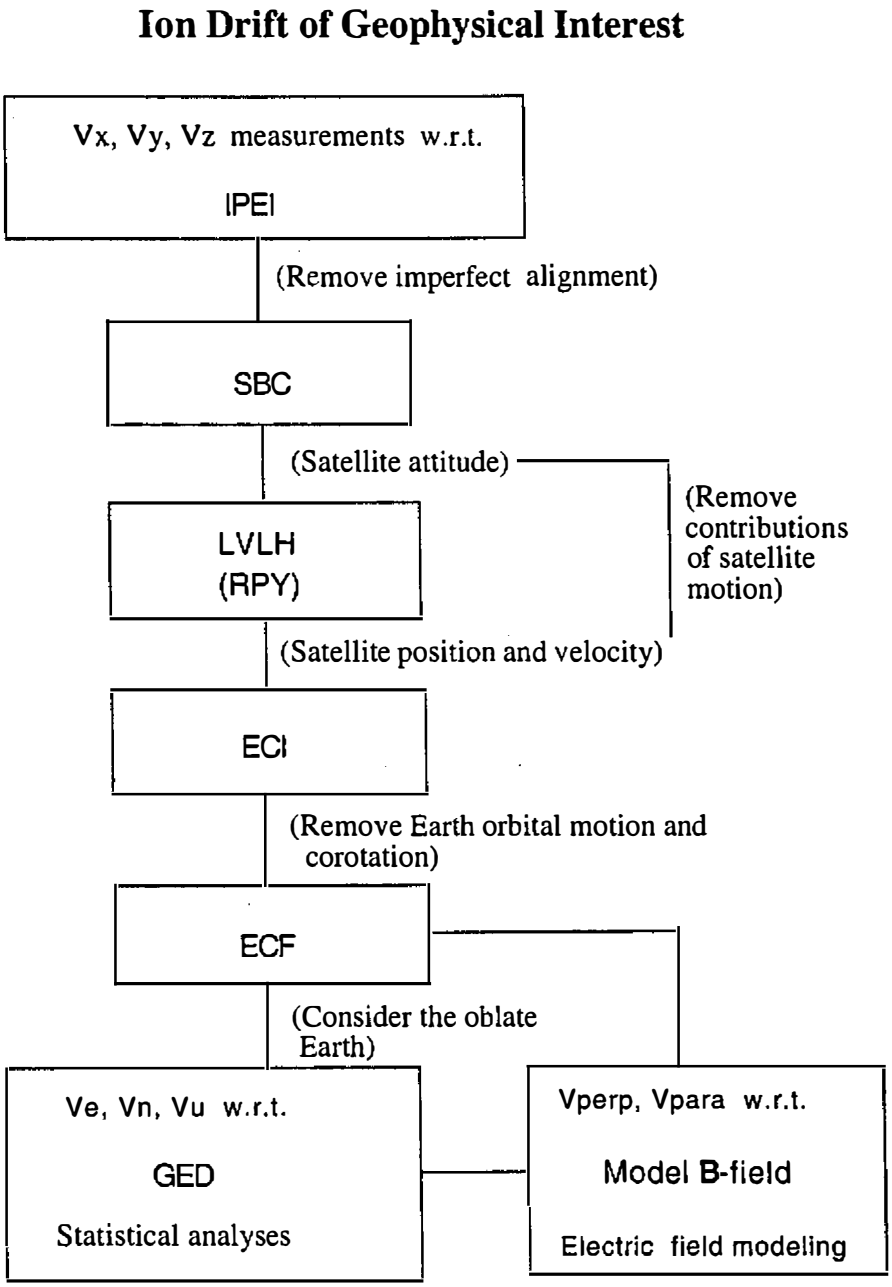

Fig. 2. Coordinate transforms required to derive ion drift vectors of geophysical interest: the instrument (IPEI), spacecraft bus coordinate (SBC), local vertical and local horizontal (LVLH) or roll-pitch-yaw (RPY) coordinate, and earth-centered inertial (ECI), earth-centered fixed (ECF) and the geodetic (GED) coordinate systems.

coordinates. For these reasons, a statistical study of ion drift in the geodetic (geographic) coordinate frame will be postponed until we have polished the modeling algorithms for the RPA data to obtain a larger data set of V_x.

3. VERTICAL DRIFT OBSERVATIONS

Vertical plasma drifts play an important role in the electrodynamics of the low-latitude ionosphere [e.g., Fejer, 1991, 1997] and have significant effects on the generation and evolution of equatorial plasma irregularities [Kil and Heelis, 1998; Fejer et al., 1999]. Here we analyze four months (March-June, 1999) of ion vertical drift (V_z) data from ROCSAT-1 to study their statistical patterns. As the contributions from satellite motion and the earth's corotation to the V_z values in the sensor reference frame are expected to be small, we will not perform the coordinate transforms on the V_z data, but will treat the IPEI V_z data directly as the drift measurements of the component parallel to the Z-axis of the geodetic frame. It is noted, however, that a positive V_z indicates a downward flow in the IPEI frame. In the following figures, we plot $-V_z$ as the vertical coordinate such that the upward direction corresponds to the upward flow. Moreover, since V_z is approximately perpendicular to the geomagnetic field at equatorial latitudes, the statistical pattern of V_z is essentially equivalent to the statistical pattern of zonal electric field there.

3.1 Data Base

As ROCSAT-1 orbits can cycle through all solar local times and geographic longitudes every 52 days, and since IPEI is operated nearly at a 100% duty cycle, the set of V_z data collected during the four months is just large enough to investigate the local time and longitudinal variations. The four-month data set is first separated according to the Kp index into quiet time ($Kp < 3$) and disturbed time ($Kp > 4+$) subsets. The disturbed time data set is fairly small and has data gaps for some longitudes and local times. Though detailed analyses of the disturbed time data set will not be performed, this data set will be used for reference whenever needed. The quiet time data set, on the other hand, has good data coverage over all longitudes and local times. This data set is further categorized according to their corrected geomagnetic latitudes (CGM) [Gustaffsson et al., 1992] into groups for the equatorial latitudes ($|CGM| < 5^o$), the equatorial ionization anomaly (EIA) latitudes ($10^o < |CGM| < 20^o$) and the low-middle latitudes ($20^o < |CGM| < 50^o$). These latitude ranges are applied to both geomagnetic hemispheres. Further separation of the data sets by solar flux conditions will not be possible using only the four-month data.

3.2 Local Time Variations of V_z at Equatorial Latitudes

To investigate the local time variations, the equatorial latitudes data sets are further grouped separately into 48 local time bins. The data are averaged in each of the 0.5-hour bins. Figure 3 presents these averaged V_z values as a function of local time for both quiet time and disturbed time conditions. Coarsely, the vertical drifts are upward in the daytime and downward

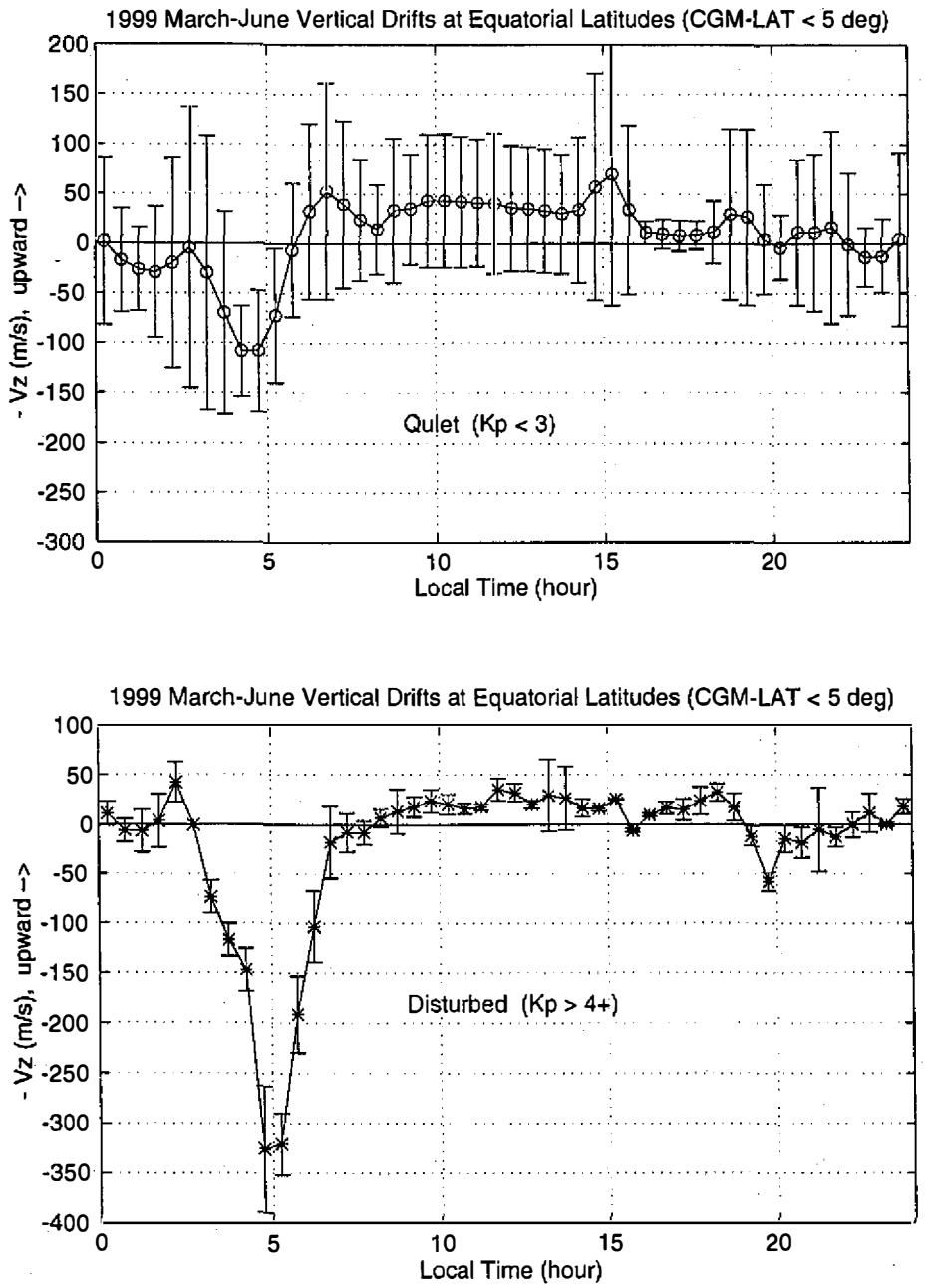

Fig. 3. Local time variations of the averaged ion vertical drifts observed at equatorial latitudes (within $\pm 5^{o}$ CGM) during March to June, 1999. Quiet (Kp < 3) geomagnetic condition (top) and disturbed (Kp > 4+) condition (bottom). Large error bars in the quiet pattern probably reflect the embedded longitudinal effects.

at nighttime for both quiet and disturbed conditions if we discount the local time bins that have small data number in the case of disturbed condition. Nighttime downward drifts during the disturbed conditions generally have larger amplitudes than those during the quiet time conditions. In contrast, the daytime upward drifts have larger amplitudes during the quiet conditions. The local time variations of the quiet time pattern are most pronounced near the terminators. Unusually large downward drifts are found at dawn (near sunrise local time). These perhaps result in a larger average value of V_z than that reported by other observations [e.g., Fig. 4 of Scherliess and Fejer, 1999]. Examining the coincident RPA I-V spectra, we found that the proton (H^+) is usually the dominant ion species where large downward drifts are measured. In the H^+ rich plasma, the measurements of ion drift meters are less accurate if the H^+ repeller were not applied. Looking into the evening features of the quiet time pattern, upward drifts were seen to extend beyond 2200 hours LT. It is difficult to uniquely determine the evening reversal time from this pattern. This probably results from the fact that we include the large upward drifts associated with spread F structures into the statistics to compute the average values.

Figure 4 presents another view of the statistical pattern of vertical drift as a function of local time by excluding the vertical drift measurements associated with proton-rich ($H^+\% > 80\%$) and spread F structures from the quiet time data set. If we allowed the deviations resulting from altitudinal, seasonal and solar activity dependencies, the characteristics of Fig. 4 more closely resemble those reported by Scherliess and Fejer [1999] who based their research on a much larger set of Jicarmarca radar and AE-E satellite data. In Fig. 4 the morning (dawn) reversal from the nighttime downward drift to the daytime upward drift occurs at about 0530 LT and the evening (dusk) reversal occurs at 1930 LT. The daytime maximum drift is seen between 0900 and 1200 LT with amplitudes of 25-30 m/s. These values agree well with those of Scherliess and Fejer [1999] who concluded that the morning reversal times and the daytime drift have little dependence on altitude or solar activity. The prereversal enhancements (~ 12 m/s) were seen at around 1830 LT. The amplitudes of these prereversal enhancements are considerably smaller than the other equatorial ground-based observations at lower altitudes and at selected longitudes. The evening vertical drifts and reversal times are expected to have large variations with longitude, solar flux, and season during the solar maximum conditions. The discrepancies between the ROCSAT-1 and other observations may be resolved when we have a larger data set.

3.3 Evening Prereversal Vertical Drift Enhancement and Equatorial Fast Rising Bubbles

Many studies have related the generation of equatorial spread F structures at early night hours with the prereversal enhancement of evening plasma vertical drifts. Hanson et al. [1997] have suggested that irregularity formation in the lower F region during a period of post sunset enhanced electric fields (upward vertical drift) will cause magnetic flux tubes of depleted plasma to accelerate upward to explain the observations of fast rising bubbles by DMSP satellites at an altitude of 800 km. Furthermore, Fejer et al. [1999] based their study on the observations of the 3-m equatorial spread F irregularities over Jicarmarca to conclude that upward drift velocities larger than about 15-20 m/s can lift the bottomside unstable layer to

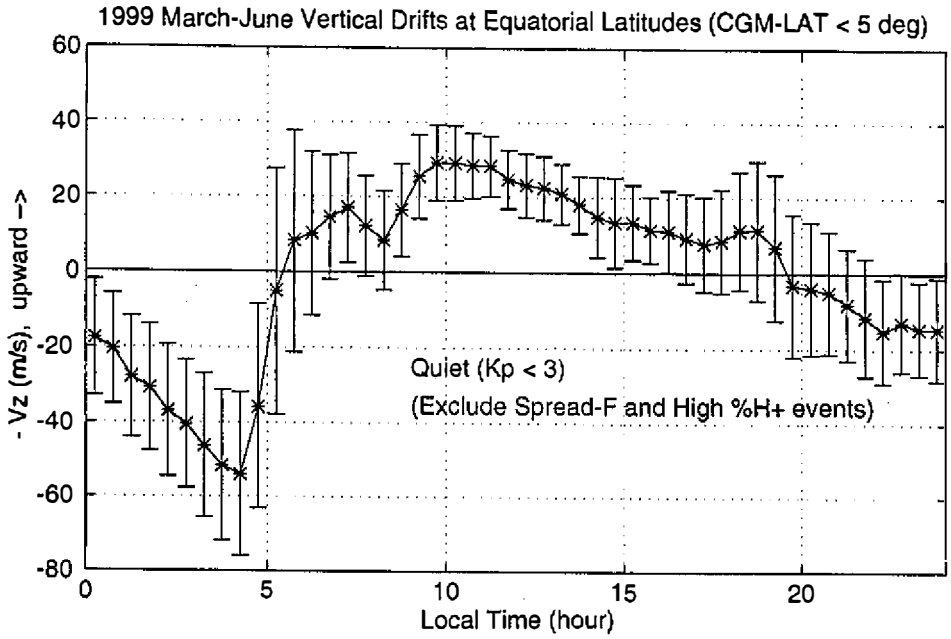

Fig. 4. Local time variations of the averaged equatorial ion vertical drifts under quiet geomagnetic conditions. The observations at the positions where H^+% exceeds 80% and where density depletion structure is present, are excluded from the database of Figure 3 for the statistics. The local times of the morning reversal and the evening reversal with prereversal enhancement can be identified from the figure. Peak daytime drifts occur between 0900 and 1200 LT.

altitudes where the gravitational drift term is dominant in the growth rate of the Rayleigh-Taylor instability. The evolution of this instability leads to wide and strong scattering regions and often gives rise to radar plumes (bubbles) extending into the topside ionosphere. The peak upward drift velocities required for the generation of strong spread F, however, depend on the solar flux conditions (e.g., about 40-45 m/s for F10.7-cm =200). It is therefore interesting to examine whether the correlation between the evening prereversal enhancement of vertical drift and the occurrence of fast rising bubbles exists at the ROCSAT-1 altitude (600 km).

Two time intervals which are under approximately the same solar flux conditions (with average F10.7-cm =105) are selected for this study. During the first interval, 20 March to 29 March 1999, ROCSAT-1 observed fast rising bubbles on almost all passes. In contrast, only a few bubble structures were observed during the second time interval, 20 April to 29 April 1999. Figure 5 presents the scatter plots of vertical drift versus local time in the 1700 to 2100 LT range for the two selected time intervals. The scatter plot for the second interval (right panel of Fig. 5) does not include the data of the passes where ROCSAT-1 saw bubble structures. The left panel is characterized by the large upward drifts associated with fast rising bubbles riding on the downward turning background drift at local times later than 1900 LT.

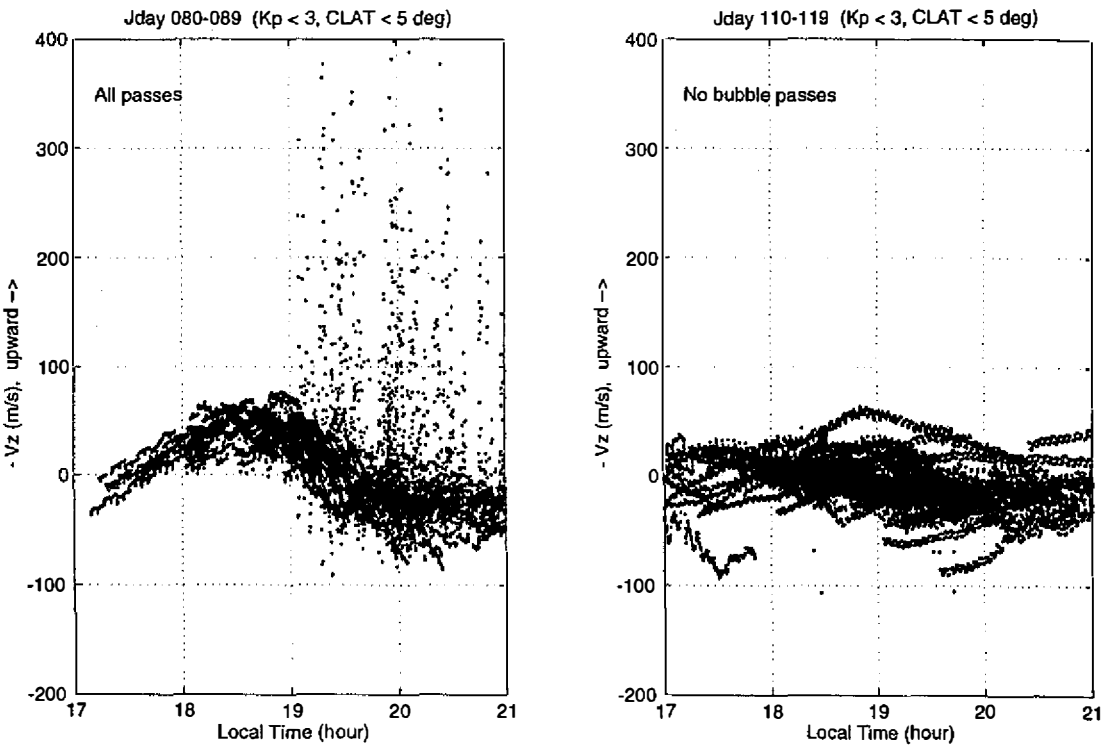

Fig. 5. Correlation of the prereversal upward drift enhancement with the occurrence of fast bubbles (characterized by the large upward V_z) in the evening local time sector (1700 - 2100 LT). Prereversal enhancements of 30-60 m/s are noticeable in the left panel but not the right.

The drift reversals all occur at local times of about 1900 to 1930 LT. The upward ion drifts at local times (around 1830 LT) about 0.5 hours prior to the reversals were enhanced to a level of about 30-60 m/s. In contrast, we do not see the bulk upward drift enhancement in the right panel. Figure 5 reconfirms that the evening upward drift enhancement can be a precursor signature of the fast rising bubbles. As fast rising bubbles most likely consist of intense small-scale irregularities (e.g., as in Yeh et al, 1999), they may significantly perturb radio signals, and thus place constraints on communication links.

3.4 Longitudinal Variations at Dawn

As noted in Figs. 3 and 4, the vertical drift patterns vary greatly at dawn (i.e., 0400 - 0600 LT). In particular, the magnitudes of downward flow near the morning reversal are much larger than those observed by the AE satellite and the Jicarmarca radar at lower altitudes and in the more limited longitude range. Since ROCSAT-1 has good data coverage over longitudes, we further examine the longitudinal variations of the vertical drift patterns in the dawn sector. Figure 6 is a scatter plot of the quiet time equatorial vertical drift as a function of longitude.

From this plot we found that the morning vertical drift reversal times are within the 0400 to 0600 LT range for almost all longitudes. Large downward drift is seen at the longitudes between 50°W and 100°E where the geomagnetic field has the greatest variations [Gustafsson et al., 1992]. Large (200m/s) upward drifts was limited to the longitudes between 50° W and 30°E. The ion vertical drift varies greatly in both the up and down directions near the South Atlantic magnetic anomaly. With the additional composition information derived from RPA data we suggest that the large downward flow at dawn is associated with the descending H^+ of the protonsphere (or plasmasphere) originally above the ROCSAT-1 altitude. Detailed analyses of the longitudinal dependencies, in particular near the South Atlantic magnetic anomaly, will be pursued in a later paper.

3.5 Local Time Variations of Vertical Drifts at Equatorial Anomaly Latitudes

Based on the empirical locations of the equatorial ionization anomaly (EIA) regions, we define the equatorial anomaly latitudes to be discussed here as the latitudes between 10° and 20° CGM. The same latitude range is applied to both hemispheres though hemispheric asym-

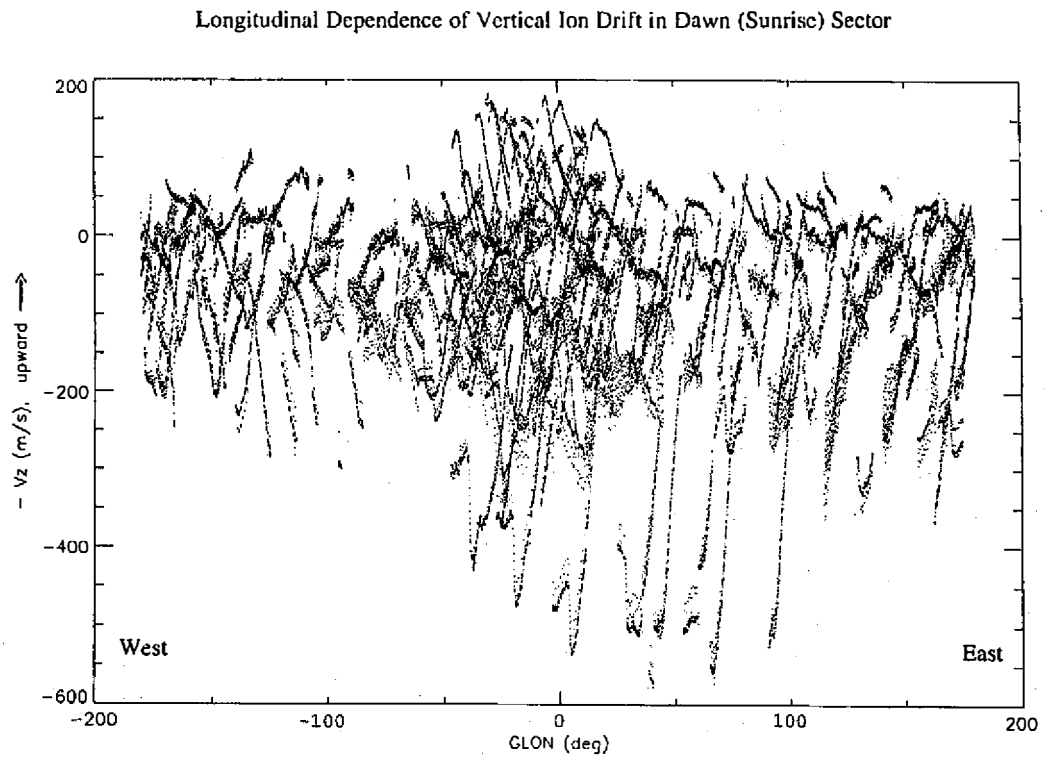

Fig. 6. Longitudinal variations of the quiet-time equatorial vertical drifts in the dawn local time sector (0400 - 0600 LT). Large upward and downward drifts are found at longitudes between 50° W and 50°E, near South Atlantic anomaly.

metry may exist. Again, the vertical drift observed at these latitudes is grouped separately into 48 local time bins for the quiet time and disturbed time conditions. The vertical drifts are averaged within each of the 48 bins. Figure 7 shows how these averaged vertical drifts vary with local times. The EIA patterns are essentially similar to the equatorial patterns shown in Fig. 3, except for the local times between 1500 and 2200 LT. Since the equatorial fast rising bubbles are most often seen in the evening hours, while the off-equator ionization anomalies are most pronounced in the late afternoon, the differences between the two patterns in the afternoon to post sunset hours may be expected.

We further separate the quiet-time EIA vertical drift data by hemisphere to examine the magnetic field control and seasonal effect on their local time variations. The resultant patterns of the vertical drift versus local time are presented in Fig. 8. As can be seen, remarkable differences exist between the northern and southern hemisphere patterns. In the local time hours from 1500 LT through midnight to dawn, the southern hemisphere vertical drift is all downward. On the other hand, the northern hemisphere vertical drift is upward and weaker. At EIA latitudes the geomagnetic field has significantly larger dip angles, and has different configurations in the different hemispheres. The ion vertical velocity has drift components parallel and perpendicular to the geomagnetic field. As the EIA phenomenon is the result of a fountain effect, we expect to see downward ion motion along the magnetic field lines at the crest EIA latitudes. The differences between the northern and southern hemisphere patterns may reflect the seasonal variations of the EIA ion motion, that is, the EIA ions are more dynamic in the fall and winter seasons. They may also reflect the asymmetrical locations of the EIA regions with respect to the magnetic equator. To obtain more significant statistics of the EIA ion dynamics, we need to include the three-component measurements (V_x, V_y, and V_z) of the drift vectors and describe the drift velocities in a geomagnetic field-oriented coordinate system.

4. SUMMARY

Using ion vertical drift data obtained in only four months from IPEI, we have validated several statistical features at equatorial latitudes, that were derived from the accumulated radar and satellite data over long duration. These include the local time dependence, longitudinal variations and geomagnetic activity dependence of ion vertical drift.

A good correlation between the post-sunset upward drift enhancements and the occurrence of fast bubbles at pre-midnight local times is found in the IPEI data. The threshold enhancement of the upward vertical drifts may be treated as a precursor signature of the formation of intense small-scale plasma irregularities in the upper ionosphere. The prediction of the occurrence of fast bubbles is an interesting subject of space weather research. It is therefore important to find out the critical values of the prereversal vertical drift enhancement required for the occurrence of fast rising bubbles under various space environment conditions, once more data can be added to the statistics.

The origin of large downward ion flow observed at sunrise local time and at longitudes near the South Atlantic magnetic anomaly is worth further investigation. The details of the

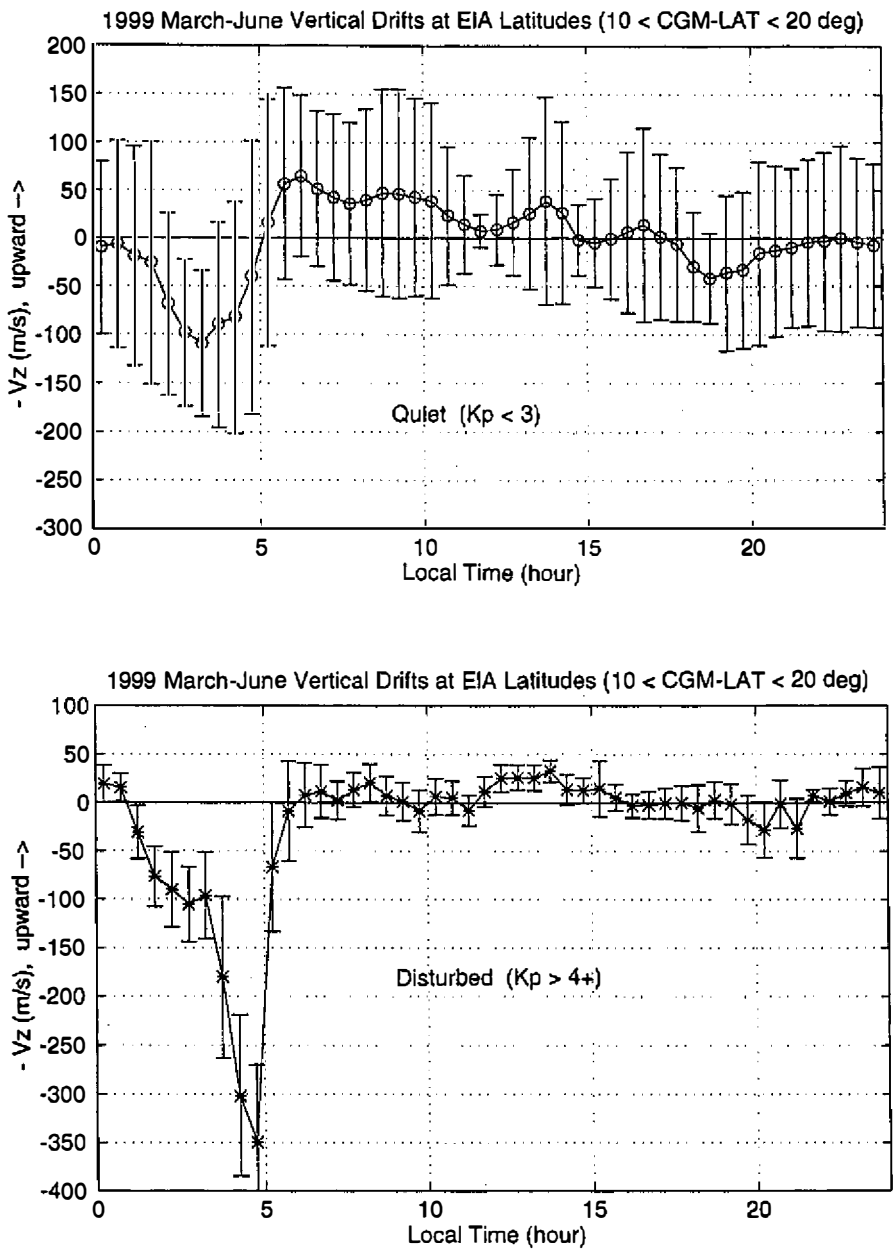

Fig. 7. Local time variations of the averaged ion vertical drifts observed at the equatorial ionization anomaly (EIA) latitudes (10^{o} - 20^{o} CGM) of both hemispheres. Noticeable differences exist between the equatorial patterns of Figure 3 and the EIA patterns in the late afternoon through premidnight hours.

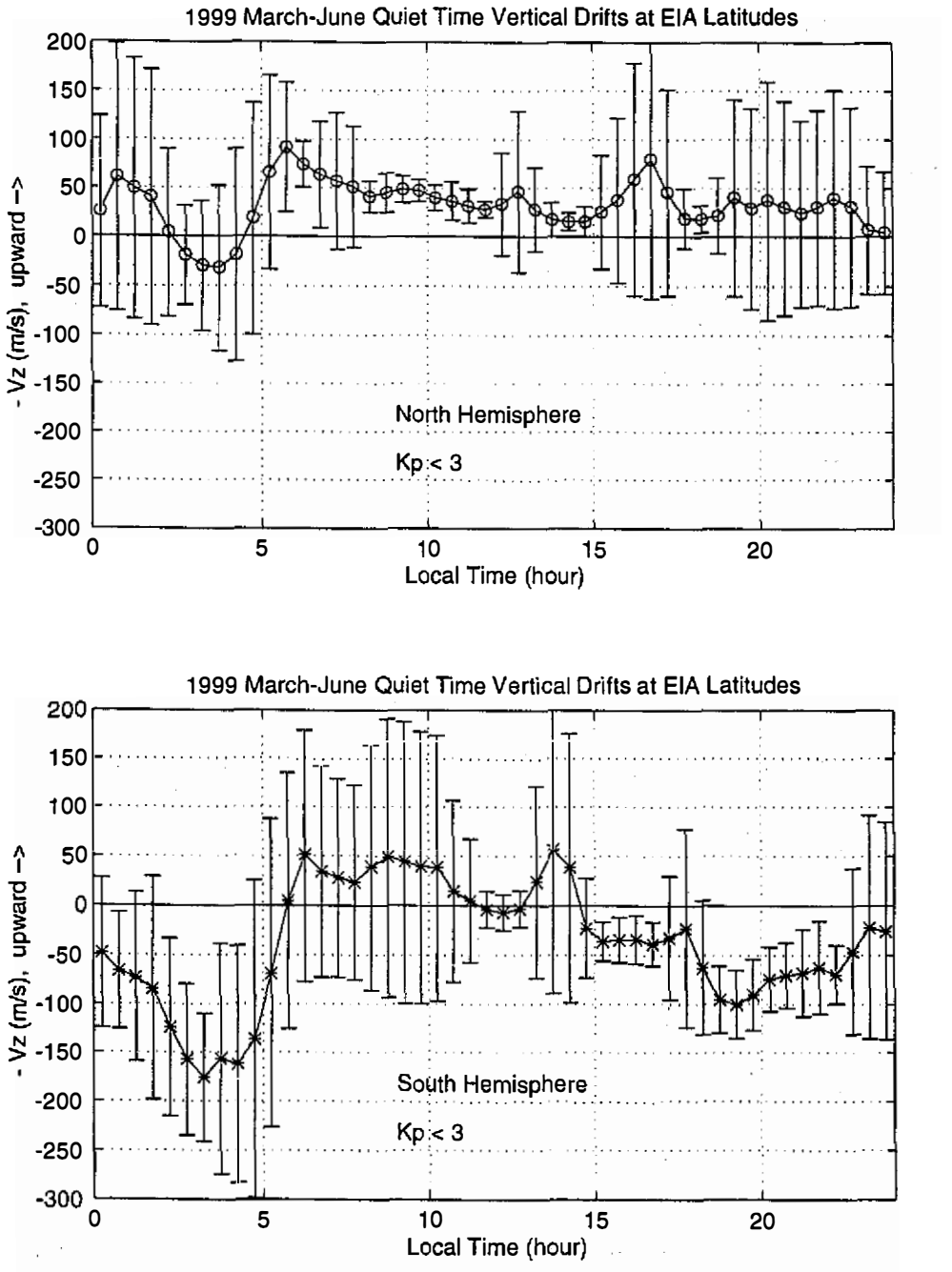

Fig. 8. Hemisphere dependence of the quiet-time vertical drift versus local time at the EIA latitudes. The southern hemisphere pattern is stronger than, but opposite in direction to, that of the northern hemisphere in the late afternoon through the nighttime hours.

longitudinal dependence of ion drift for all local times will be studied to take advantage of good longitudinal coverage of the ROCSAT-1 orbit.

Due to its 35° inclination orbital motion, the ROCSAT-IPEI can provide, probably for the first time, a large set of ion velocity data over the equatorial ionization anomaly (EIA) regions. We are interested in identifying the statistical features of ion drift at the EIA latitudes since previous observations at these latitudes are scarce. The observed hemispherical dependence of the EIA ion drift patterns suggests the necessity of taking seasonal effects into consideration, and of resolving the ion drift vectors into their components which are perpendicular and parallel to the geomagnetic field, before any further statistical analysis is pursued.

A larger data set is required to improve our investigations of the disturbed-time statistics and the solar flux dependency of ion drift patterns. As the IPEI data are accumulated we will continue the statistical analyses of ion drift data to understand better the controlling parameters and processes of the statistical patterns.

Acknowledgments This report has been supported by National Space Program Office Operation Contract NSC89-NSPO(A)-PDD-008-STP01 and by National Science Council Research Project NSC89-2111-M-008-027-AP9.

REFERENCES

Coley, W. R., and R. A. Heelis, 1989: Low-latitude zonal and vertical ion drifts seen by DE-2. *J. Geophys. Res.*, **94**, 6751-6761.

Fejer, B. G., 1991: Low latitude electrodynamics plasma drift: A review. *J. Atmos. Terr. Phys.*, **53**, 677-693.

Fejer, B. G., E. R. de Paula, R. A. Heelis, and W. B. Hanson, 1995: Global equatorial ionospheric vertical plasma drifts measured by AE-E satellite. *J. Geophys. Res.*, **100**, 5769-5776.

Fejer, B. G., E. R. de Paula, and L. Scherliess, 1999: Effects of vertical plasma drift velocity on the generation and evolution of equatorial spread F. *J. Geophys. Res.*, **104**, 19859-19869.

Gustaffsson, G., N. E. Papitashvili, and V. O. Papitashvili, 1992: A revised corrected geomagnetic coordinate system for Epochs 1985 and 1990. *J. Atmos. Terr. Phys.*, **54**, 1609-1631.

Hanson, W. B., W. R. Coley, R. A. Heelis, and A. L. Urquhart, 1997: Fast equatorial bubbles. *J. Geophys. Res.*, **102**, 2039-2045.

Hanson, W. B., and R. A. Heelis, 1975: Techniques for measuring bulk gas-motion from satellites. *Space Sci. Instrum.*, **1**, 493.

Kil, H., and R. A. Heelis, 1998: Equatorial density irregularity structures at intermediate scales and their temporal evolution. *J. Geophys. Res.*, **103**, 3969-3981.

Scherliess, L., and B. G. Fejer, 1999: Radar and satellite global equatorial F region vertical drift model. *J. Geophys. Res.*, **104**, 6829-6842.

Su, S. Y., H. C. Yeh, R. A. Heelis, J. M. Wu, S. C. Yang, L. F. Lee, and S. L. Chen,1999: The

ROCSAT-1 IPEI preliminary results: low-latitude ionospheric plasma and flow variations. *TAO*, **10**, 787-804.

Yeh, H. C., 1998: Characteristics of the IPEI payload onboard ROCSAT-1, National Central University internal report: IPEI-NCU-98-R-1.1, March.